Energy & Environmental Science

Cite this: *Energy Environ. Sci.*, 2012, **5**, 5686

www.rsc.org/ees

COMMUNICATION

Borohydride hydrazinates: high hydrogen content materials for hydrogen storage†

Teng He,[a] Hui Wu,[bc] Guotao Wu,[a] Junhu Wang,[a] Wei Zhou,[bc] Zhitao Xiong,[a] Juner Chen,[a] Tao Zhang[a] and Ping Chen*[a]

Received 17th November 2011, Accepted 7th December 2011
DOI: 10.1039/c2ee03205h

A new class of hydrogen storage materials, borohydride hydrazinates, was successfully synthesized. In particular, the bidentate NH_2NH_2 coordinates with $LiBH_4$ in molar ratios of 1 : 1 and 1 : 2 giving rise to a monoclinic $LiBH_4 \cdot NH_2NH_2$ and orthorhombic $LiBH_4 \cdot 2NH_2NH_2$, respectively. Around 13.0 wt% H_2 can be released from $LiBH_4 \cdot NH_2NH_2$ at 140 °C in the presence of Fe–B catalysts.

Development of safe and energy efficient hydrogen storage materials is one of the technical challenges towards the large scale utilization of hydrogen energy.[1] In the past, tremendous efforts have been given to light-weight complex/chemical hydrides, including borohydrides,[2] alanates,[3] amides,[4] ammonia borane,[5] metal amidoboranes[6] *etc.* Among them, $LiBH_4$ has received close attention due to its high hydrogen content (18.4 wt%); however, its potential use in automotive applications is compromised by the unfavorable thermodynamics for dehydrogenation, *i.e.*, with an enthalpy of *ca.* 67 kJ mol^{-1} $LiBH_4$ can only decompose to H_2 in a stepwise manner at temperatures above 300 °C.[7] Thermodynamic alterations *via* compositing $LiBH_4$ with MgH_2,[8] $LiNH_2$[9] or NH_3[10] *etc.* have been investigated, among which $LiBH_4$ has been found to form complexes with $LiNH_2$ or NH_3 forming Li_2BNH_6,[11] $Li_4BN_3H_{10}$[12] or $LiBH_4 \cdot xNH_3$,[10b,13] respectively, leading to the remarkable changes in the dehydrogenation thermodynamics, *i.e.*, from a highly endothermic to a mild exothermic nature. The co-existence of $H^{\delta+}$ (in NH_3 or NH_2^-) and $H^{\delta-}$ (in BH_4^-) in these systems has been proven to effectively facilitate hydrogen release.[10a,14] It is, therefore, of particular interest to probe the combination of other $H^{\delta+}$ rich compounds such as hydrazine with borohydrides, and thus, to improve dehydrogenation properties.

Hydrazine (NH_2NH_2), a commonly used spacecraft propellant, contains 12.5 wt% of hydrogen and decomposes *via* two competing pathways giving rise to H_2, N_2 and NH_3 under mild conditions with the help of noble or noble metal-like catalysts.[15] Recent results from Singh and Xu showed that the decomposition of hydrazine hydrate catalyzed by bimetallic nanoparticles achieved nearly 100% selectivity to hydrogen and nitrogen at room temperature.[16] Hydrazine can also complex with borane forming $N_2H_4 \cdot BH_3$[17] and $N_2H_4 \cdot 2BH_3$, where $N_2H_4 \cdot BH_3$ decomposes to H_2 at a temperature range of 100–150 °C. As there are two lone pair electrons at N's, N_2H_4 is capable of binding the metal cation of borohydrides through two donor sites, and forming hydrazinates. Meanwhile, the co-existence of $H^{\delta+}$ and $H^{\delta-}$ is expected to facilitate dehydrogenation from the system. In the present study several hydrazinates of $LiBH_4$, $NaBH_4$, and $Mg(BH_4)_2$, were synthesized successfully. In particular, NH_2NH_2 adducts strongly to $LiBH_4$ in 1/1 or 1/2 molar ratios, resulting in monoclinic $LiBH_4 \cdot NH_2NH_2$ and orthorhombic $LiBH_4 \cdot 2NH_2NH_2$, respectively.

[a] *Dalian Institute of Chemical Physics, Chinese Academy of Sciences, 457, Zhongshan Road, Dalian, China. E-mail: pchen@dicp.ac.cn; Fax: +86-411-84379583; Tel: +86-411-84379905*
[b] *NIST Center for Neutron Research, National Institute of Standards and Technology, Gaithersburg, Maryland, 20899-6102, USA*
[c] *Department of Materials Science and Engineering, University of Maryland, College Park, Maryland, 20742-2115, USA*

† Electronic supplementary information (ESI) available. Experimental details, XRD, XAFS, FT-IR, Raman, ^{57}Fe Mössbauer results *etc.* CCDC reference numbers [CCDC NUMBER(S)]. For ESI and crystallographic data in CIF or other electronic format see DOI: 10.1039/c2ee03205h

Broader context

Lack of safe and efficient hydrogen storage materials is one of the pending issues in the implementation of hydrogen fuel cell technology. Tremendous efforts have been given to the development of materials with high hydrogen content. Herein, a new type of hydrogen storage material, namely lithium borohydride hydrazinate, was successfully synthesized by ball milling $LiBH_4$ and NH_2NH_2. In particular, NH_2NH_2 complexes with $LiBH_4$ in molar ratios of 1/1 and 2/1 giving rise to a monoclinic $LiBH_4 \cdot NH_2NH_2$ and an orthorhombic $LiBH_4 \cdot 2NH_2NH_2$, respectively. Importantly, around 13.0 wt% hydrogen can be released from $LiBH_4 \cdot NH_2NH_2$ at 140 °C with the assistance of an Fe-based catalyst. Spectroscopic analyses (Mössbauer and XAFS) evidence that an Fe–B amorphous alloy is the functional catalytic species. To the best of our knowledge, this is the first report on the synthesis and dehydrogenation of borohydride hydrazinates.

More importantly, around 13.0 wt% hydrogen can be released from the Fe-catalyzed $LiBH_4 \cdot NH_2NH_2$ at 140 °C. To the best of our knowledge, this is the first report on the synthesis and direct dehydrogenation of borohydride hydrazinates.

The reaction of hydrazine with $LiBH_4$ in various molar ratios (2/1, 1/1 and 1/2), yields a series of new phases (shown in Fig. S1†). Similarly, treating $NaBH_4$ and $Mg(BH_4)_2$ with hydrazine can also result in the corresponding new hydrazinate compounds (Fig. S2 and S3†). The Fourier transform infrared (FTIR) and Raman spectra show the presence of a vibration at around 1120 cm^{-1} (Fig. S4 and S5†) assignable to the N–N stretching,[18] which evidences the retention of the N–N bonding in the hydrazinates. The X-ray diffraction (XRD) patterns of $LiBH_4 \cdot NH_2NH_2$ and $LiBH_4 \cdot 2NH_2NH_2$ samples were indexed using, respectively, a monoclinic *Cc* cell and an orthorhombic $Pca2_1$ cell with lattice parameters of $a = 12.1423$ Å, $b = 6.7217$ Å, $c = 10.3680$ Å, $\beta = 104.79°$, and $a = 12.0638$ Å, $b = 6.5219$ Å, $c = 7.6983$ Å. The crystal structures are shown in Fig. 1, and the Rietveld fits to the diffraction patterns are shown in Fig. S6 and S8†. In $LiBH_4 \cdot NH_2NH_2$ each Li^+ is surrounded by two BH_4^- ions and two NH_2NH_2 molecules with the Li–B distances of 2.322–2.600 Å and the Li–N distances of 2.131–2.427 Å, leading to a distorted tetrahedral coordination (Fig. S7†). In the structure of $LiBH_4 \cdot 2NH_2NH_2$, each Li^+ is tetrahedrally coordinated by four NH_2NH_2 molecules forming a tetrahydrazinelithium $[Li(N_2H_4)_4](I)$ complex cation with Li–N distances of 1.962–2.248 Å. Having lone pairs on two N's, N_2H_4 is a bidentate ligand and can act as a bridge to link the neighboring $[Li(N_2H_4)_4]^+$ tetrahedra through edge-sharing, forming a chain-like cationic complex of $[Li(NH_2NH_2)_2]^+$. Such $[Li(NH_2NH_2)_2]^+$ chains are then separated by the free BH_4^- anions (Fig. 1), as in the structure of $[Li_2(H_2N–NHMe)_3](BH_4)_2$.[19]

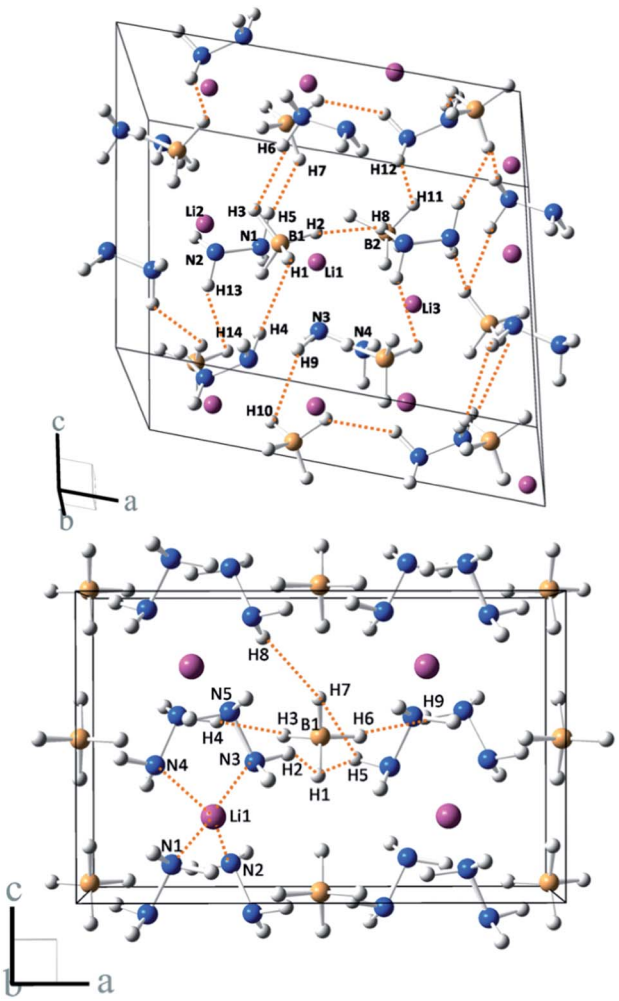

Fig. 1 Crystal structures of $LiBH_4 \cdot NH_2NH_2$ (top) and $LiBH_4 \cdot 2NH_2NH_2$ (bottom). The N–H···H–B dihydrogen bonds are highlighted in orange dash lines. Li, B, N and H atoms are represented by purple, yellow, blue and gray spheres, respectively.

Both $LiBH_4 \cdot NH_2NH_2$ and $LiBH_4 \cdot 2NH_2NH_2$ contain oppositely charged $H^{\delta+}$ (in N_2H_4) and $H^{\delta-}$ (in BH_4^-), hence the interactions between these H's result in the elongated N–H and B–H distances compared to those in the neat $LiBH_4$[20] and NH_2NH_2.[21] From the crystal structures, the H's in N_2H_4 have short distances to their neighboring H in BH_4^-, ranging from 2.066 to 2.323 Å in $LiBH_4 \cdot NH_2NH_2$, and from 1.926 to 2.397 Å in $LiBH_4 \cdot 2NH_2NH_2$, respectively, which indicates the establishment of dihydrogen bonding (see Tables 1, S1 and S2†). In particular, the shortest $H^{\delta+} \cdots H^{\delta-}$ distance (1.926 Å) in $LiBH_4 \cdot 2NH_2NH_2$ system is even less than those in any other B–N containing hydrogenous compounds.[2c,22] Similar to the dihydrogen bonding in ammonia borane,[5a,22b] which is primarily responsible for the stability of this molecular crystal at room temperature, the entire network of the intermolecular dihydrogen bonding in the hydrazinates, together with the interactions between Li^+ and NH_2NH_2/BH_4^- (Fig. 1), is thus the main driving force for the structural stabilization and is expected to have a profound impact on their thermal decomposition.

Dehydrogenation properties of $LiBH_4 \cdot NH_2NH_2$ and $LiBH_4 \cdot 2NH_2NH_2$ were analyzed by volumetric release and mass spectrometry (MS) measurements (Fig. 2). Decomposition of hydrazine follows two competing routes: *i.e.*, to N_2 and H_2 (reaction 1, denoted hereafter as eqn (1)) and to N_2 and NH_3 (reaction 2, eqn (2)).[15a–c]

$$N_2H_4 \rightarrow N_2 + 2H_2 \quad (1)$$

$$3N_2H_4 \rightarrow N_2 + 4NH_3 \quad (2)$$

Volumetric release and MS measurements show that (Fig. 2) neat hydrazine releases 0.1 equiv. gas per hydrazine at 140 °C in 17 h, which is mainly composed of NH_3 and N_2 (see MS signals in Fig. S9†), following eqn (2).[15a] Neat $LiBH_4$ hardly releases H_2 under this condition. However, the $LiBH_4 \cdot NH_2NH_2$ sample decomposes at temperatures right above 110 °C and releases *ca.* 0.55 equiv. gas comprised of N_2, NH_3 and a significant amount of H_2 (molar ratio of $H_2/N_2 = 0.94$) at 140 °C (shown in Fig. 2). $LiBH_4 \cdot 2NH_2NH_2$ starts to decompose at about 75 °C and evolves more than 1.5 equiv. gas per $LiBH_4$ under the same condition. The gaseous product is also a mixture of N_2, NH_3 and H_2 (Fig. S10†). The presence of significant amount of N_2 and NH_3 in both hydrazinates in comparison with neat N_2H_4 indicates the "catalytic role" of $LiBH_4$ in eqn (2), which manifests in the elongated N–H and N–N bonds in NH_2NH_2 units of the hydrazinates. The formation of H_2, on the other hand, may not be *via* the self-decomposition of the "activated" hydrazine following eqn (1), which is evidenced by the observation of B–N species in the solid residue by ^{11}B magic angle spinning nuclear magnetic resonance (MAS NMR) (Fig. S11†). Moreover, only H_2, no N_2 (Fig. S13†), can

Table 1 Interatomic distances (Å) in $LiBH_4 \cdot NH_2NH_2$ and $LiBH_4 \cdot 2NH_2NH_2$ compared with pristine hydrazine and $LiBH_4$ at room temperature[a]

	$LiBH_4 \cdot NH_2NH_2$	$LiBH_4 \cdot 2NH_2NH_2$	NH_2NH_2	$LiBH_4$
B···H	1.217–1.231[a]	1.225–1.234	—	1.208–1.225
N···H	1.025–1.036	1.030	1.021	—
N···N	1.447–1.452	1.452	1.449	—
Li···B	2.322–2.600	3.735–4.426	—	2.475–2.542
Li···N	2.131–2.427	1.962–2.248	—	—
Shortest $H^{\delta+}\cdots H^{\delta-}$	2.066	1.926	—	—

[a] Close contacts around the Li^+ center in $LiBH_4 \cdot NH_2NH_2$ and interatomic distances can be found in the ESI†.

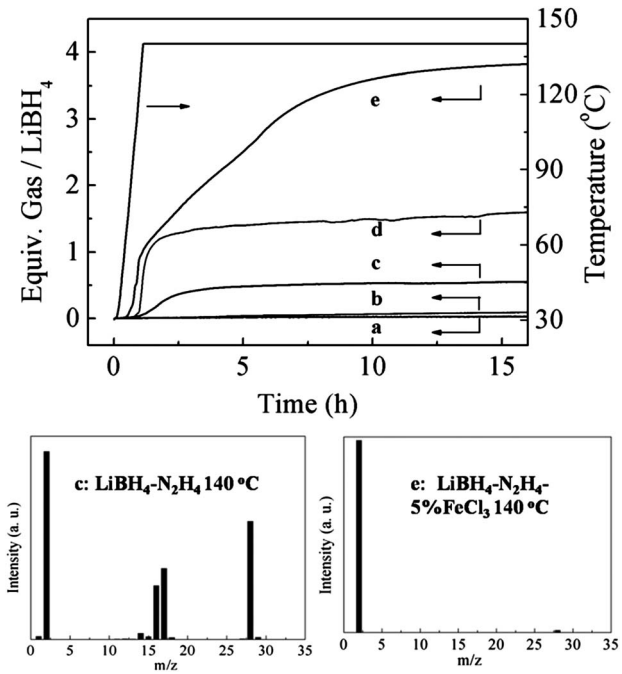

Fig. 2 Volumetric release measurements (top) on neat $LiBH_4$ (a), hydrazine (b), $LiBH_4 \cdot NH_2NH_2$ (c), $LiBH_4 \cdot 2NH_2NH_2$ (d), and 5.0 mol% $FeCl_3$-doped $LiBH_4 \cdot NH_2NH_2$ (e) at 140 °C. The gas evolution from hydrazine is quantified by equiv. gas/hydrazine. MS profiles (bottom) of the gaseous products of $LiBH_4 \cdot NH_2NH_2$ (c) and 5.0 mol% $FeCl_3$-doped $LiBH_4 \cdot NH_2NH_2$ (e) upon heating them at 140 °C.

be released from $LiBH_4 \cdot 1/3NH_2NH_2$ at 140 °C (Fig. S12†), further excluding the occurrence of the self-decomposition of NH_2NH_2 (eqn (1)) We propose that the formation of H_2 is more likely *via* the interaction of $LiBH_4$ and N_2H_4. Note that the dissociation of the N–N bond is easier than that of the N–H bond in hydrazine;[23] NH_2NH_2 may first dissociate homogeneously into two neutral [$\cdot NH_2$] radicals, which, then, abstract electrons from H^- of BH_4^- giving rise to $LiNH_2BH_3$ and H_2. $LiNH_2BH_3$ can readily decompose to H_2 under the same condition mentioned above.[24] Another possible pathway proposed here resembles the "hydride-transfer" mechanism in the decomposition of amidoboranes,[25] in which one hydride in BH_4^- transfers to Li^+ giving rise to the intermediates LiH and BH_3, which further interact with hydrazine to form $LiH/BH_3NH_2NH_2$. It was reported that $BH_3NH_2NH_2$ or $LiH/BH_3NH_2NH_2$ released hydrogen easily under mild conditions.[17a] More detailed investigation on this aspect is underway.

The primary objective of the present study is to convert both H in BH_4^- and NH_2NH_2 to H_2. The limited decomposition of hydrazinates shown above evidences the presence of a kinetic barrier. We, thus, introduced 5 mol% of $FeCl_3$ to $LiBH_4 \cdot NH_2NH_2$ to examine its catalytic effect.[26] As shown in Fig. 2, gas evolution was observed at ~60 °C, which is much lower than that of pristine $LiBH_4 \cdot NH_2NH_2$. More than 3.8 equiv. gaseous products/$LiBH_4$ can be released at 140 °C, which contain mainly H_2 and N_2 (Fig. 2) with a molar ratio of 12/1 (GC result). Therefore 13.0 wt% hydrogen (~88% of the hydrogen content) is released from the Fe-catalyzed $LiBH_4 \cdot NH_2NH_2$ sample. Heating the sample to 250 °C results in more than 4 equiv. total gas per $LiBH_4$ (corresponding to 13.8 wt% H_2) (Fig. S14†). Notably, the concentration of NH_3 is lower than 0.1 mol% in the gaseous phase detected by a conductivity meter. XRD patterns of the post-dehydrogenated $FeCl_3$-doped $LiBH_4 \cdot NH_2NH_2$ sample reveal the formation of BN (Fig. S16†). In addition, FTIR and Raman spectra show the disappearance of B–H and N–H vibrational modes and the appearance of BN_2^{3-} and B–N modes instead (Fig. S17 and S18†). Summarizing the above information, the overall decomposition of $LiBH_4 \cdot NH_2NH_2$ in the presence of the Fe-based catalyst may follow eqn (3).

$$3(LiBH_4 \cdot N_2H_4) \rightarrow Li_3BN_2 + 2BN + N_2 + 12H_2 \quad (3)$$

It is reported that Fe, Co and Ni are efficient catalysts for the decomposition of B–N–H compounds.[27] Ferric or ferrous salts can be easily reduced by BH_3 or BH_4^- to form an amorphous Fe–B alloy.[27b,28] In this work, the formation of an Fe–B alloy is evidenced by the X-ray absorption fine structure (XAFS) and ^{57}Fe Mössbauer analyses (ESI†). Fe in both samples is essentially in the reduced state (XANES spectra shown in Fig. S19†) with a broad peak to the first shell atoms (Fourier transform structure shown in Fig. S20†), which is in good agreement with the feature of the amorphous Fe–B alloy reported previously.[27b] The ^{57}Fe Mössbauer spectrum on the $FeCl_3$-doped $LiBH_4 \cdot NH_2NH_2$ sample clearly shows an isomer shift (IS) at 0.17 mm s^{-1}, which is close to those of $Fe_{44}Co_{19}B_{37}$, $Fe_{62}B_{38}$ and Fe–B alloys reported in the literature[27b,28] and is similar to the ball milled 5 mol% $FeCl_3$–$LiBH_4$ sample (Fig. S21 and Table S3†). It is likely that the Fe–B alloy is the functional species catalyzing the dehydrogenation of $LiBH_4 \cdot N_2H_4$.

The presence of the catalyst may significantly alter the dehydrogenation pathway. For instance, transition metals of the first row of the periodic table were found to be highly effective in catalyzing eqn (2) under the condition applied here. It is likely that hydrazine first decomposes to N_2 and NH_3, and NH_3 molecules derived then coordinate with $LiBH_4$ to form $LiBH_4$ ammoniate, which was observed in the solid residue (Fig. S22†). Our recent work showed that in the presence of the Co–B alloy, $LiBH_4 \cdot (4/3)NH_3$ can directly dehydrogenate in the temperature range of 140–250 °C and form Li_3BN_2 and

BN.[14] It was found that the Fe–B alloy exhibits a similar catalytic performance. In this context, N_2 and NH_3 should be the main components in the gaseous phase in the initial stage of decomposition. Another possibility is that the dehydrogenation is *via* the direct combination of $H^{\delta+}$ (in N_2H_4) and $H^{\delta-}$ (in BH_4^-) with the aid of the Fe–B alloy, where H_2 and N_2 could evolve simultaneously. To investigate the exact dehydrogenation pathway, gaseous products collected in the initial stage of decomposition (from 59 to 90 °C) were analyzed by mass spectrometry (Fig. S23†). It was found that although H_2 was the dominant species, the signal intensities of H_2, N_2, and NH_3 increased simultaneously with temperature, indicating the likelihood of concurrence of both dehydrogenation paths mentioned above.

Conclusions

The coordination of the bidentate ligand hydrazine to the metal centers in borohydrides leads to the formation of a series of new borohydride hydrazinate compounds. The binding between metals and hydrazine and the interactions between the protonic H in NH_2NH_2 and hydridic H in the BH_4^- ions "catalyze" the decomposition of hydrazine. With the aid of the Fe–B catalyst, ~13.0 wt% hydrogen was evolved from $LiBH_4 \cdot NH_2NH_2$ at a temperature as low as 140 °C, which makes the borohydride hydrazinate a compelling candidate for hydrogen storage. However, the formation of Li_3BN_2 and BN in the final products indicates the direct rehydrogenation is impossible.[9a] Thus, regeneration of hydrazinates off-board from the spent fuel is, thus, a subject of further study. More investigations are also needed to elucidate dehydrogenation mechanisms and to optimize the dehydrogenation property of the hydrazinates.

Acknowledgements

We would like to acknowledge the financial supports from the Hundred Talents Project and Knowledge Innovation Program of CAS (KGCX2-YW-806 and KJCX2-YW-H21) and 973 (2010CB631304) Project. XAFS and high resolution XRD experiments were performed in Shanghai Synchrotron Radiation Facility.

Notes and references

1 (*a*) P. Chen and M. Zhu, *Mater. Today*, 2008, **11**, 36; (*b*) L. Schlapbach and A. Züttel, *Nature*, 2001, **414**, 353; (*c*) C. Weidenthaler and M. Felderhoff, *Energy Environ. Sci.*, 2011, **4**, 2495; (*d*) http://www1.eere.energy.gov/hydrogenandfuelcells/storage/.
2 (*a*) A. Züttel, P. Wenger, S. Rentsch, P. Sudan, P. Mauron and C. Emmenenegger, *J. Power Sources*, 2003, **118**, 1; (*b*) R. Černý, Y. Filinchuk, H. Hagemann and K. Yvon, *Angew. Chem., Int. Ed.*, 2007, **46**, 5765; (*c*) S.-i. Orimo, Y. Nakamori, J. R. Eliseo, A. Züttel and C. M. Jensen, *Chem. Rev.*, 2007, **107**, 4111; (*d*) Y. Guo, H. Wu, W. Zhou and X. Yu, *J. Am. Chem. Soc.*, 2011, **133**, 4690.
3 B. Bogdanović and M. Schwickardi, *J. Alloys Compd.*, 1997, **253–254**, 1.
4 P. Chen, Z. Xiong, J. Luo, J. Lin and K. L. Tan, *Nature*, 2002, **420**, 302.
5 (*a*) A. Staubitz, A. P. M. Robertson and I. Manners, *Chem. Rev.*, 2010, **110**, 4079; (*b*) A. Gutowska, L. Li, Y. Shin, C. M. Wang, X. S. Li, J. C. Linehan, R. S. Smith, B. D. Kay, B. Schmid, W. Shaw, M. Gutowski and T. Autrey, *Angew. Chem., Int. Ed.*, 2005, **44**, 3578; (*c*) M. G. Hu, R. A. Geanangel and W. W. Wendlandt, *Thermochim. Acta*, 1978, **23**, 249.
6 (*a*) Z. Xiong, C. K. Yong, G. Wu, P. Chen, W. Shaw, A. Karkamkar, T. Autrey, M. O. Jones, S. R. Johnson, P. P. Edwards and W. I. F. David, *Nat. Mater.*, 2008, **7**, 138; (*b*) H. V. K. Diyabalanage, R. P. Shrestha, T. A. Semelsberger, B. L. Scott, M. E. Bowden, B. L. Davis and A. K. Burrell, *Angew. Chem., Int. Ed.*, 2007, **46**, 8995.
7 A. Züttel, S. Rentsch, P. Fischer, P. Wenger, P. Sudan, P. Mauron and C. Emmenegger, *J. Alloys Compd.*, 2003, **356–357**, 515.
8 (*a*) T. E. C. Price, D. M. Grant, V. Legrand and G. S. Walker, *Int. J. Hydrogen Energy*, 2010, **35**, 4154; (*b*) J. J. Vajo, S. L. Skeith and F. Mertens, *J. Phys. Chem. B*, 2005, **109**, 3719.
9 (*a*) F. E. Pinkerton, G. P. Meisner, M. S. Meyer, M. P. Balogh and M. D. Kundrat, *J. Phys. Chem. B*, 2004, **109**, 6; (*b*) T. Noritake, M. Aoki, S. Towata, A. Ninomiya, Y. Nakamori and S. Orimo, *Appl. Phys. A: Mater. Sci. Process.*, 2006, **83**, 277.
10 (*a*) Y. Guo, G. Xia, Y. Zhu, L. Gao and X. Yu, *Chem. Commun.*, 2010, **46**, 2599; (*b*) S. R. Johnson, W. I. F. David, D. M. Royse, M. Sommariva, C. Y. Tang, F. P. A. Fabbiani, M. O. Jones and P. P. Edwards, *Chem.–Asian J.*, 2009, **4**, 849.
11 (*a*) H. Wu, W. Zhou, T. J. Udovic, J. J. Rush and T. Yildirim, *Chem. Mater.*, 2008, **20**, 1245; (*b*) P. A. Chater, W. I. F. David and P. A. Anderson, *Chem. Commun.*, 2007, 4770.
12 (*a*) Y. E. Filinchuk, K. Yvon, G. P. Meisner, F. E. Pinkerton and M. P. Balogh, *Inorg. Chem.*, 2006, **45**, 1433; (*b*) P. A. Chater, W. I. F. David, S. R. Johnson, P. P. Edwards and P. A. Anderson, *Chem. Commun.*, 2006, 2439.
13 E. A. Sullivan and S. Johnson, *J. Phys. Chem.*, 1959, **63**, 233.
14 X. Zheng, G. Wu, W. Li, Z. Xiong, T. He, J. Guo, H. Chen and P. Chen, *Energy Environ. Sci.*, 2011, **4**, 3593.
15 (*a*) X. Chen, T. Zhang, M. Zheng, Z. Wu, W. Wu and C. Li, *J. Catal.*, 2004, **224**, 473; (*b*) M. Zheng, X. Chen, R. Cheng, N. Li, J. Sun, X. Wang and T. Zhang, *Catal. Commun.*, 2006, **7**, 187; (*c*) J. P. Contour and G. Pannetier, *J. Catal.*, 1972, **24**, 434; (*d*) L. Ding, Y. Shu, A. Wang, M. Zheng, L. Li, X. Wang and T. Zhang, *Appl. Catal., A*, 2010, **385**, 232.
16 (*a*) S. K. Singh and Q. Xu, *J. Am. Chem. Soc.*, 2009, **131**, 18032; (*b*) S. K. Singh and Q. Xu, *Chem. Commun.*, 2010, **46**, 6545.
17 (*a*) T. Hügle, M. F. Kühnel and D. Lentz, *J. Am. Chem. Soc.*, 2009, **131**, 7444; (*b*) J. Hannauer, O. Akdim, U. B. Demirci, C. Geantet, J. Herrmann, P. Miele and Q. Xu, *Energy Environ. Sci.*, 2011, **4**, 3355.
18 J. R. Durig and C. Zheng, *Vib. Spectrosc.*, 2002, **30**, 59.
19 J. C. Gálvez Ruiz, H. Nöth and M. Warchhold, *Eur. J. Inorg. Chem.*, 2008, **2008**, 251.
20 M. R. Hartman, J. J. Rush, T. J. Udovic, R. C. Bowman, Jr and S.-J. Hwang, *J. Solid State Chem.*, 2007, **180**, 1298.
21 K. Kohata, T. Fukuyama and K. Kuchitsu, *J. Phys. Chem.*, 1982, **86**, 602.
22 (*a*) G. Soloveichik, J.-H. Her, P. W. Stephens, Y. Gao, J. Rijssenbeek, M. Andrus and J. C. Zhao, *Inorg. Chem.*, 2008, **47**, 4290; (*b*) W. T. Klooster, T. F. Koetzle, P. E. M. Siegbahn, T. B. Richardson and R. H. Crabtree, *J. Am. Chem. Soc.*, 1999, **121**, 6337; (*c*) H. Chu, G. Wu, Z. Xiong, J. Guo, T. He and P. Chen, *Chem. Mater.*, 2010, **22**, 6021; (*d*) H. Wu, W. Zhou and T. Yildirim, *J. Am. Chem. Soc.*, 2008, **130**, 14834.
23 (*a*) M. Szwarc, *Proc. R. Soc. London, Ser. A*, 1949, **198**, 267; (*b*) S. Foner, *J. Chem. Phys.*, 1958, **29**, 442; (*c*) I. P. Fisher and G. A. Heath, *Nature*, 1965, **208**, 1199.
24 Z. Xiong, C. K. Yong, G. Wu, P. Chen, W. Shaw, A. Karkamkar, T. Autrey, M. O. Jones, S. R. Johnson, P. P. Edwards and W. I. F. David, *Nat. Mater.*, 2008, **7**, 138.
25 (*a*) D. Y. Kim, N. J. Singh, H. M. Lee and K. S. Kim, *Chem.–Eur. J.*, 2009, **15**, 5598; (*b*) T. B. Lee and M. L. McKee, *Inorg. Chem.*, 2009, **48**, 7564–7575; (*c*) A. T. Luedtke and T. Autrey, *Inorg. Chem.*, 2010, **49**, 3905.
26 Note: Reducing Fe-based catalyst loading from 5 mol% to 2 mol% will also bring significant kinetic improvement.
27 (*a*) W. S. Tang, G. Wu, T. Liu, A. T. S. Wee, C. K. Yong, Z. Xiong, A. T. S. Hor and P. Chen, *Dalton Trans.*, 2008, 2395; (*b*) T. He, J. Wang, G. Wu, H. Kim, T. Proffen, A. Wu, W. Li, T. Liu, Z. Xiong, C. Wu, H. Chu, J. Guo, T. Autrey, T. Zhang and P. Chen, *Chem.–Eur. J.*, 2010, **16**, 12814.
28 (*a*) J. van Wonterghem, S. Morup, C. J. W. Koch, S. W. Charles and S. Wells, *Nature*, 1986, **322**, 622; (*b*) T. He, J. Wang, T. Liu, G. Wu, Z. Xiong, J. Yin, H. Chu, T. Zhang and P. Chen, *Catal. Today*, 2011, **170**, 69.